

Dynamical holographic QCD model: resembling renormalization group from ultraviolet to infrared

Danning Li and Mei Huang

Abstract Resembling the renormalization group from ultraviolet (UV) to infrared (IR), we construct a dynamical holographic model in the graviton-dilaton-scalar framework, where the dilaton background field Φ and scalar field X are responsible for the gluodynamics and chiral dynamics, respectively. At the UV boundary, the dilaton field is dual to the dimension-4 gluon operator, and the scalar field is dual to the dimension-3 quark-antiquark operator. The metric structure at IR is automatically deformed by the nonperturbative gluon condensation and chiral condensation in the vacuum. The produced scalar glueball spectra in the graviton-dilaton framework agree well with lattice data, and the light-flavor meson spectra generated in the graviton-dilaton-scalar framework are in well agreement with experimental data. Both the chiral symmetry breaking and linear confinement are realized in this dynamical holographic QCD model. The necessary condition for the existence of linear quark potential is discussed, and the pion form factor is also investigated in the dynamical hQCD model.

1 Introduction

Quantum chromodynamics (QCD) is accepted as the fundamental theory of the strong interaction. In the ultraviolet (UV) or weak coupling regime of QCD, the perturbative calculations agree well with experiment. However, in the infrared (IR) regime, the description of QCD vacuum as well as hadron properties and processes

Danning Li
Institute of High Energy Physics, Chinese Academy of Sciences, Beijing 100049
e-mail: lidn@mail.ihep.ac.cn

Mei Huang (speaker)
Institute of High Energy Physics, Chinese Academy of Sciences, Beijing 100049
e-mail: huangm@mail.ihep.ac.cn

in terms of quark and gluon still remains as outstanding challenge in the formulation of QCD as a local quantum field theory.

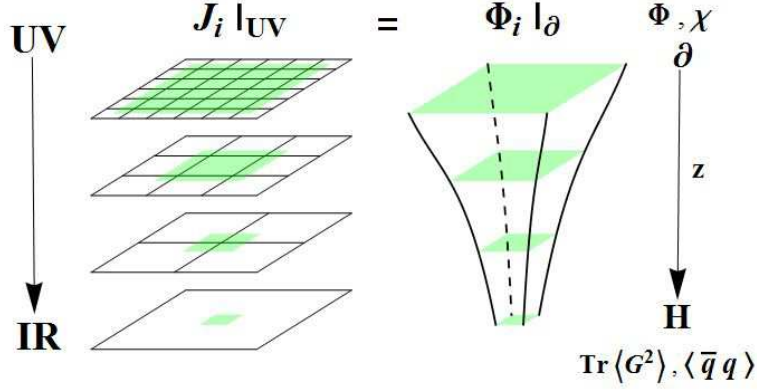


Fig. 1 Duality between d -dimension QFT and $d+1$ -dimension gravity as shown in [8] (Left-hand side). Dynamical holographic QCD model resembles RG from UV to IR (Right-hand side): at UV boundary the dilaton bulk field $\Phi(z)$ and scalar field $X(z)$ are dual to the dimension-4 gluon operator and dimension-3 quark-antiquark operator, which develop condensates at IR.

In order to derive the low-energy hadron physics and understand the deep-infrared sector of QCD from first principle, various non-perturbative methods have been employed, in particular lattice QCD, Dyson-Schwinger equations (DSEs), and functional renormalization group equations (FRGs). In recent decades, an entirely new method based on the anti-de Sitter/conformal field theory (AdS/CFT) correspondence and the conjecture of the gravity/gauge duality [1, 2, 3] provides a revolutionary method to tackle the problem of strongly coupled gauge theories. Though the original discovery of holographic duality requires supersymmetry and conformality, the holographic duality has been widely used in investigating hadron physics [4, 5, 6, 7], strongly coupled quark gluon plasma and condensed matter. It is widely believed that the duality between the quantum field theory and quantum gravity is an unproven but true fact. In general, holography relates quantum field theory (QFT) in d -dimensions to quantum gravity in $(d+1)$ -dimensions, with the gravitational description becoming classical when the QFT is strongly-coupled. The extra dimension can be interpreted as an energy scale or renormalization group (RG) flow in the QFT [8] as shown in Fig.1.

In this talk, we introduce our recently developed dynamical holographic QCD model [9], which resembles the renormalization group from ultraviolet (UV) to infrared (IR). The dynamical holographic model is constructed in the graviton-dilaton-scalar framework, where the dilaton background field $\Phi(z)$ and scalar field $X(z)$ are responsible for the gluodynamics and chiral dynamics, respectively. At the UV

boundary, the dilaton field $\Phi(z)$ is dual to the dimension-4 gluon operator, and the scalar field $X(z)$ is dual to the dimension-3 quark-antiquark operator. The metric structure at IR is automatically deformed by the nonperturbative gluon condensation and chiral condensation in the vacuum. In Fig.1, we show the dynamical holographic QCD model, which resembles the renormalization group from UV to IR.

2 Pure gluon system: Graviton-dilaton framework

For the pure gluon system, we construct the quenched dynamical holographic QCD model in the graviton-dilaton framework by introducing one scalar dilaton field $\Phi(z)$ in the bulk. The 5D graviton-dilaton coupled action in the string frame is given below:

$$S_G = \frac{1}{16\pi G_5} \int d^5x \sqrt{g_s} e^{-2\Phi} (R_s + 4\partial_M \Phi \partial^M \Phi - V_G^s(\Phi)). \quad (1)$$

Where G_5 is the 5D Newton constant, g_s , Φ and V_G^s are the 5D metric, the dilaton field and dilaton potential in the string frame, respectively. The metric ansatz is often chosen to be

$$ds^2 = b_s^2(z)(dz^2 + \eta_{\mu\nu} dx^\mu dx^\nu), \quad b_s(z) \equiv e^{A_s(z)}. \quad (2)$$

To avoid the gauge non-invariant problem and to meet the requirement of gauge/gravity duality, we take the dilaton field in the form of

$$\Phi(z) = \mu_G^2 z^2 \tanh(\mu_{G^2}^4 z^2 / \mu_G^2). \quad (3)$$

In this way, the dilaton field at UV behaves $\Phi(z) \xrightarrow{z \rightarrow 0} \mu_{G^2}^4 z^4$, and is dual to the dimension-4 gauge invariant gluon operator $\text{Tr}G^2$, while at IR it takes the quadratic form $\Phi(z) \xrightarrow{z \rightarrow \infty} \mu_G^2 z^2$. By self-consistently solving the Einstein equations, the metric structure will be automatically deformed at IR by the dilaton background field, for details, please refer to [9].

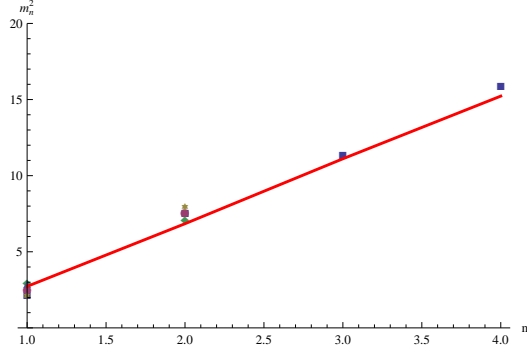
We assume the glueball can be excited from the QCD vacuum described by the quenched dynamical holographic model, and the 5D action for the scalar glueball $\mathcal{G}(x, z)$ in the string frame takes the form as

$$S_{\mathcal{G}} = \int d^5x \sqrt{g_s} \frac{1}{2} e^{-\Phi} [\partial_M \mathcal{G} \partial^M \mathcal{G} + M_{\mathcal{G},5}^2 \mathcal{G}^2]. \quad (4)$$

The Equation of motion for \mathcal{G} has the form of

$$-e^{-(3A_s - \Phi)} \partial_z (e^{3A_s - \Phi} \partial_z \mathcal{G}_n) = m_{\mathcal{G},n}^2 \mathcal{G}_n. \quad (5)$$

Fig. 2 The scalar glueball spectra for the dilaton field $\Phi(z) = \mu_G^2 z^2 \tanh(\mu_{G^2}^4 z^2 / \mu_G^2)$ with $\mu_G = \mu_{G^2} = 1 \text{ GeV}$. The dots are lattice data taken from [10].



After the transformation $\mathcal{G}_n \rightarrow e^{-\frac{1}{2}(3A_s - \Phi)} \mathcal{G}_n$, we get the schrodinger like equation of motion for the scalar glueball

$$-\mathcal{G}_n'' + V_{\mathcal{G}} \mathcal{G}_n = m_{\mathcal{G},n}^2 \mathcal{G}_n, \quad (6)$$

with the 5D effective schrodinger potential

$$V_{\mathcal{G}} = \frac{3A_s'' - \Phi''}{2} + \frac{(3A_s' - \Phi')^2}{4}. \quad (7)$$

Then from Eq. (6), we can solve the scalar glueball spectra and the result is shown in Fig.2. It is a surprising result that if one self-consistently solves the metric background under the dynamical dilaton field, it gives the correct ground state and at the same time gives the correct Regge slope.

Following the standard procedure, the heavy quark potential $V_{Q\bar{Q}}$ and the interquark distance $R_{Q\bar{Q}}$ can be worked out. We also find the necessary condition for the linear quark potential: There exists a point z_c , at which $b_s'(z_c) \rightarrow 0, b_s(z_c) \rightarrow \text{const}$, then one can obtain the string tension

$$\sigma_s \propto \frac{V_{Q\bar{Q}}(z_0)}{R_{\bar{q}q}(z_0)} \xrightarrow{z_0 \rightarrow z_c} \frac{L^2}{2\pi\alpha_p} b_s^2(z_c). \quad (8)$$

Where α_p is the 5D string tension. From the left-hand figure in Fig.3, we can see that only for the case of positive dilaton background $\Phi = \mu_G^2 z^2$ and $\Phi = \mu_G^2 z^2 \tanh(\mu_{G^2}^4 z^2 / \mu_G^2)$, the metric has a minimum point z_c . Correspondingly, the quark-antiquark potential indeed shows a linear part for positive quadratic dilaton background $\Phi = \mu_G^2 z^2$ and for $\Phi = \mu_G^2 z^2 \tanh(\mu_{G^2}^4 z^2 / \mu_G^2)$ as shown in right-hand figure in Fig.3. While for the pure AdS₅ case as well as for the dynamical soft-wall model with negative dilaton background field $\Phi = -\mu_G^2 z^2$, there doesn't exist a z_c where $b_s'(z_c) \rightarrow 0$, and correspondingly the heavy quark potential does not show a linear behavior at large z .

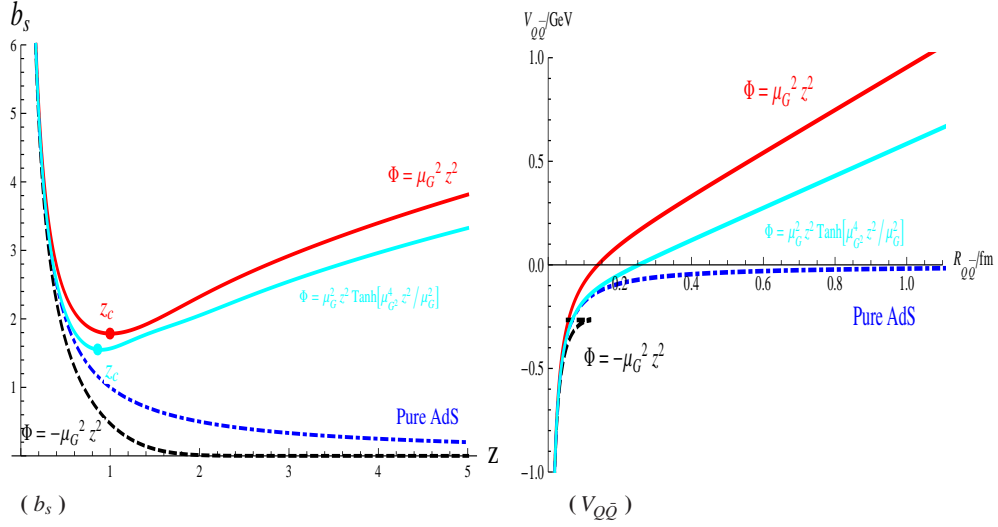


Fig. 3 The metric structure $b_s(z) = e^{A_s(z)}$ as functions of z (left-hand side), and the quenched quark potential result $V_{Q\bar{Q}}$ as functions of $R_{Q\bar{Q}}$ (right-hand side) corresponding to $\Phi = \mu_G^2 z^2$ (red solid line), $\Phi = -\mu_G^2 z^2$ (black dashed line), and $\Phi = \mu_G^2 z^2 \tanh(\mu_G^4 z^2 / \mu_G^2)$ (green solid line), respectively. The blue dash-dotted line stands for the pure AdS₅ case. $\mu_G = 1 \text{ GeV}$ has been taken for numerical calculation.

3 Dynamical holographic QCD model for meson spectra

We then add light flavors in terms of meson fields on the gluodynamical background. The total 5D action for the graviton-dilaton-scalar system takes the following form:

$$S = S_G + \frac{N_f}{N_c} S_{KKSS}, \quad (9)$$

with

$$S_G = \frac{1}{16\pi G_5} \int d^5x \sqrt{g_s} e^{-2\Phi} (R + 4\partial_M \Phi \partial^M \Phi - V_G(\Phi)), \quad (10)$$

$$S_{KKSS} = - \int d^5x \sqrt{g_s} e^{-\Phi} \text{Tr}(|DX|^2 + V_X(X^+ X, \Phi)) + \frac{1}{4g_s^2} (F_L^2 + F_R^2). \quad (11)$$

In the vacuum, it is assumed that there are both gluon condensate and chiral condensate. The dilaton background field Φ is supposed to be dual to some kind of gluodynamics in QCD vacuum. We take the dilaton background field $\Phi(z) = \mu_G^2 z^2 \tanh(\mu_G^4 z^2 / \mu_G^2)$. The scalar field $X(z)$ is dual to dimension-3 quark-antiquark operator, and $\chi(z)$ is the vacuum expectation value (VEV) of the scalar field $X(z)$. For detailed analysis please refer to [9]. The equations of motion of the vector, axial-vector, scalar and pseudo-scalar mesons take the form of:

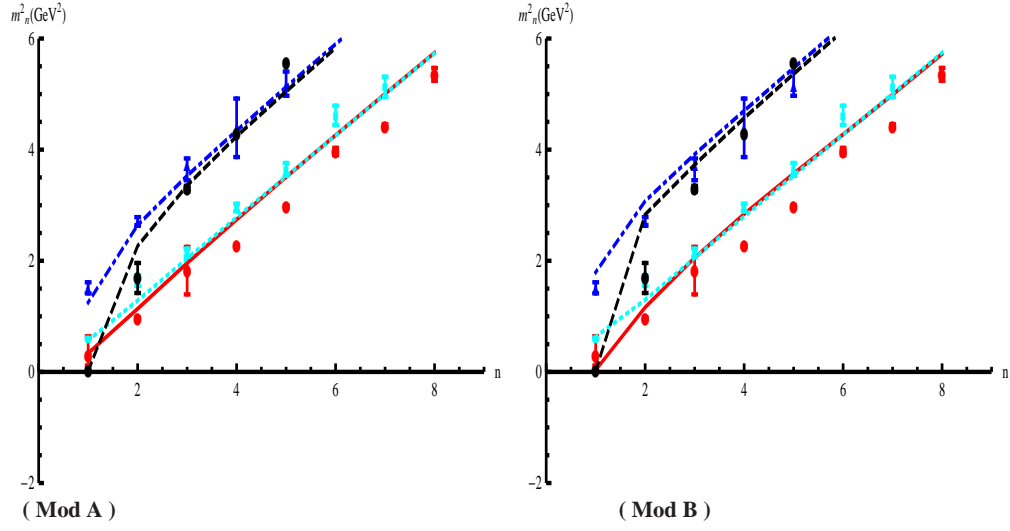


Fig. 4 Meson spectra in the dynamical soft-wall model with two sets of parameters in Table 1 comparing with experimental data. The red and black lines are for scalars and pseudoscalars, the green and blue lines are for vectors and axial-vectors.

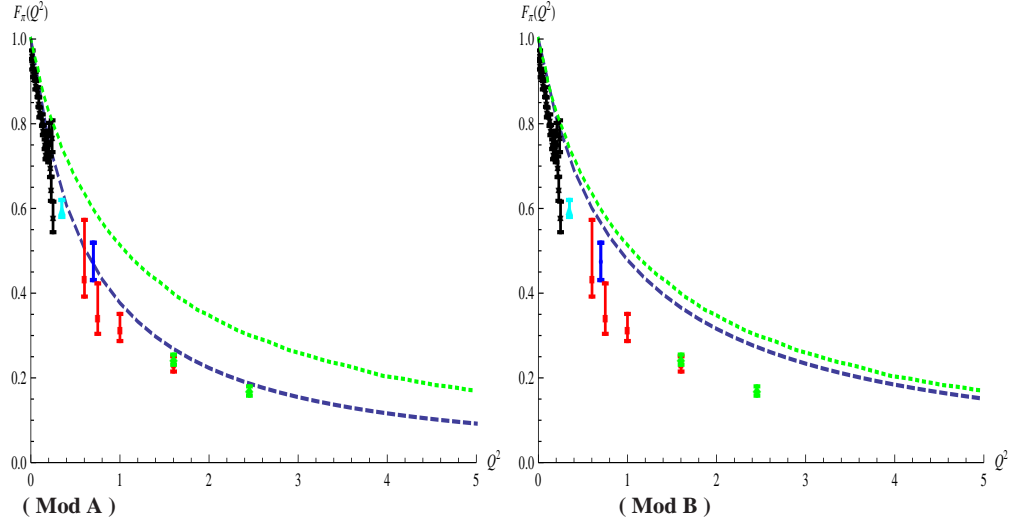


Fig. 5 $F_\pi(Q^2)$ as function of Q^2 for Mod A and B defined in Table 1 and compared with experimental data. The blue dashed lines are the prediction in our model, and the green dotted line is the original soft-wall model results taken from Ref.[11].

$$-\rho_n'' + V_\rho \rho_n = m_n^2 \rho_n, \quad (12)$$

$$-a_n'' + V_a a_n = m_n^2 a_n, \quad (13)$$

$$-s_n'' + V_s s_n = m_n^2 s_n, \quad (14)$$

$$-\pi_n'' + V_{\pi,\varphi} \pi_n = m_n^2 (\pi_n - e^{A_s} \chi \varphi_n),$$

$$-\varphi_n'' + V_\varphi \varphi_n = g_5^2 e^{A_s} \chi (\pi_n - e^{A_s} \chi \varphi_n). \quad (15)$$

with schrodinger like potentials

$$V_\rho = \frac{A'_s - \Phi'}{2} + \frac{(A'_s - \Phi')^2}{4}, \quad (16)$$

$$V_a = \frac{A'_s - \Phi'}{2} + \frac{(A'_s - \Phi')^2}{4} + g_5^2 e^{2A_s} \chi^2, \quad (17)$$

$$V_s = \frac{3A''_s - \phi''}{2} + \frac{(3A'_s - \phi')^2}{4} + e^{2A_s} V_{C,\chi\chi}(\chi, \Phi), \quad (18)$$

$$V_{\pi,\varphi} = \frac{3A''_s - \Phi'' + 2\chi''/\chi - 2\chi'^2/\chi^2}{2} + \frac{(3A'_s - \Phi' + 2\chi'/\chi)^2}{4}, \quad (19)$$

$$V_\varphi = \frac{A''_s - \Phi''}{2} + \frac{(A'_s - \Phi')^2}{4}. \quad (20)$$

For our numerical calculations, we take two sets of parameters in Table 1. The parameters in Mod A has a smaller chiral condensate, which gives a smaller pion decay constant $f_\pi = 65.7\text{MeV}$, and the parameters in Mod B has a larger chiral condensate, which gives a reasonable pion decay constant $f_\pi = 87.4\text{MeV}$.

	G_5/L^3	m_q (MeV)	$\sigma^{1/3}$ (MeV)	$\mu_G = \mu_{G^2}$
Mod A	0.75	8.4	165	0.43
Mod B	0.75	6.2	226	0.43

Table 1 Two sets of parameters.

The meson spectra and pion form factor are shown in Fig.4 and Fig. 5. It is observed that from Fig.4 that in our graviton-dilaton-scalar system, with two sets of parameters, the generated meson spectra agree well with experimental data. For the pion form factor, it is found that with parameters set A used with a smaller chiral condensate, the produced pion form factor matches the experimental data much better, however, the produced pion decay constant is much smaller than experimental data. With parameters in set B corresponding to a larger chiral condensate, one can produce better result for pion decay constant, but the results on pion form factor are worse.

4 Discussion and summary

In this work, we construct a quenched dynamical holographic QCD (hQCD) model in the graviton-dilaton framework for the pure gluon system, and develop a dynamical hQCD model for the two flavor system in the graviton-dilaton-scalar framework by adding light flavors on the gluodynamical background. The dynamical holographic model resembles the renormalization group from ultraviolet (UV) to

infrared (IR). The dilaton background field Φ and scalar field X are responsible for the gluodynamics and chiral dynamics, respectively. At the UV boundary, the dilaton field is dual to the dimension-4 gluon operator, and the scalar field is dual to the dimension-3 quark-antiquark operator. The metric structure at IR is automatically deformed by the nonperturbative gluon condensation and chiral condensation in the vacuum. The produced scalar glueball spectra in the graviton-dilaton framework agree well with lattice data, and the light-flavor meson spectra generated in the graviton-dilaton-scalar framework are in well agreement with experimental data. Both the chiral symmetry breaking and linear confinement are realized in the dynamical holographic QCD model.

We also give a necessary condition for the existence of linear quark potential from the metric structure, and we show that in the graviton-dilaton framework, a negative quadratic dilaton background field cannot produce the linear quark potential.

The pion form factor is also investigated in the dynamical hQCD model. It is found that with smaller chiral condensate, the produced pion form factor matches the experimental data much better, however, the produced pion decay constant is much smaller than experimental data. With larger chiral condensate, one can produce better result for pion decay constant, but the result on pion form factor is worse.

Acknowledgements This work is supported by the NSFC under Grant Nos. 11175251 and 11275213, DFG and NSFC (CRC 110), CAS key project KJCX2-EW-N01, K.C.Wong Education Foundation, and Youth Innovation Promotion Association of CAS.

References

1. Maldacena J. M., *Adv. Theor. Math. Phys.* **2**, 231 (1998).
2. Gubser S. S., Klebanov I. R. and Polyakov A. M., *Phys. Lett. B* **428**, 105 (1998).
3. Witten E., *Adv. Theor. Math. Phys.* **2**, 253 (1998).
4. A. Karch, E. Katz, D. T. Son and M. A. Stephanov, *Phys. Rev. D* **74** (2006) 015005.
5. C. Csaki and M. Reece, *JHEP* **0705**, 062 (2007).
6. Gherghetta T., Kapusta J. I. and Kelley T. M., *Phys. Rev. D* **79** (2009) 076003.
7. Sui Y. -Q., Wu Y. -L., Xie Z. -F. and Yang Y. -B., *Phys. Rev. D* **81** (2010) 014024; Sui Y. -Q., Wu Y. -L. and Yang Y. -B., *Phys. Rev. D* **83** (2011) 065030.
8. Adams A., Carr L. D., Schaefer T., Steinberg P. and Thomas J. E., *New J. Phys.* **14**, 115009 (2012).
9. Li D. N., Huang M. and Yan Q. -S. , *Eur.Phys.J.C*(2013) 73:2615; Li D.N, Huang M., arXiv:1303.6929[hep-ph], to appear in *JHEP*.
10. Meyer H. B., hep-lat/0508002; Lucini B. and Teper M. , *JHEP* **0106** (2001) 050; Morningstar C. J. and Peardon M. J., *Phys. Rev. D* **60** (1999) 034509; Chen Y., Alexandru A., Dong S. J., Draper T., *et al.*, *Phys. Rev. D* **73** (2006) 014516.
11. Kwee H. J. and Lebed R. F., *JHEP* **0801** (2008) 027; H. J. Kwee and R. F. Lebed, *Phys. Rev. D* **77** (2008) 115007.